Sensors & Transducers, Vol. 183, Issue 12, December 2014, pp. 215-220

Sensors & Transducers

http://www.sensorsportal.com

Performance Comparison of Two Topologies Double-Fed Brushless Machine with 36 Slots for Low-Speed Applications

Yue Hao, Huijuan Liu, Jun Wang
School of Electrical Engineering, Beijing Jiaotong University,
No. 3 Shang Yuan Cun, Beijing, 100044, China
Tel.: 18813096961, fax: 010-5168-7101
E-mail: 13121407@bjtu.edu.cn

Received: 14 August 2014 /Accepted: 28 November 2014 /Published: 31 December 2014

Abstract: The performances of two topologies of low-speed double-fed brushless machine (DFBM) with fractional slot windings are quantitatively compared and analyzed using two-dimensional (2-D) finite element method (FEM). To fairly compare the torque capability and power efficiency of different DFBMs, the investigated DFBMs have the same outer diameter, the same axial stack length and the same iron core materials, and some comparison rules are presented. In order to maximize the torque density, several important structure parameters are optimized. The results of this paper reveal the torque density levels and power density levels of two kinds of DFBMs. *Copyright © 2014 IFSA Publishing, S. L.*

Keywords: Double-fed brushless machine (DFBM), Radial magnetic field modulation, Fractional slot windings, Torque density, Power density, FEM.

1. Introduction

A double-fed brushless machine (DFBM) appears very attractive for its rugged structure (complete absence of slip rings and brushes), good compatibility with power converter, and flexible operational modes for various application needs [1, 2]. According to the flux modulated types, there are different topologies machine. One type of DFBM (referred as DFBM-I) shown in Fig. 1 (a) was stemming from the cascaded induction machine and the self-cascaded induction motor [3, 4]. This type of DFBM has two sets of separate windings with different pole numbers (2p and 2q) located on one stator, and the rotor is structured with several reluctance segments with pole number different from either of the stator windings. The operation of this machine relies on the interaction of the two stator windings through the intermediate action of the rotor [5-7].

The other type of DFBM (referred as DFBM-II) is shown in Fig. 1 (b) whose operating principle is similar to that of magnetic gears [8-10]. This proposed DFBM has one rotating part and two stationary windings with different pole numbers (2p and 2q) located on two stators respectively. The function of rotating steel segments in the air-gap is to modulate the magnetic fields produced by each of the stationary windings, resulting in appropriate space harmonics with the required pole pairs to interact with other windings to convert the mechanical power into electric power [11-13].

As far as the authors are aware, there is no quantitative comparison between the two types of proposed DFBMs. In this paper, a rule to compare the power density of the DFBMs is presented. The performance of the low-speed DFBM-I is compared with those of low-speed DFBM-II with fractional-slot windings. The stator EMF, electromagnetic torque, core losses and efficiency of the two machines have been investigated by using 2D transient finite element analysis method.

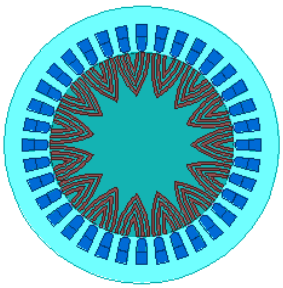

(a) DFBM-I

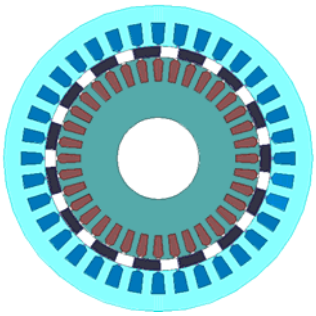

(b) DFBM-II

Fig. 1. Cross section of two types of DFBMs.

2. Comparison Rules for Two Motors

The purpose of this paper is to compare the output power per unit volume of two different types of motors. All the motors being studied have three phases and are operated as synchronous motors and double-fed motors. For the synchronous motor operation, one set of stator windings are fed with 50 Hz three-phase sinusoidal AC currents, the other set of stator windings are fed with three-phase DC currents, and the synchronous speed of two DFBMs is 200 rpm. For the double-fed motor operation, two sets of stator windings are fed with 50 Hz and 35 Hz three-phase sinusoidal AC currents respectively, and the rated speed of two DFBMs is 60 rpm. Rules to compare the power densities of two motors are:

1) Two motors have the same outside radius and axial length; the same grade of iron and copper materials, the same stator slot number for two stators, the same cross-sectional area of one slot, and the same conductor numbers per slot, the same cross-sectional area of one conductor.

2) The operation state (synchronous motor and double-fed motor) of two DFBMs are the same. The magnitudes and frequencies of two stator currents of two motors are the same, and the rotor speeds of two motors are the same.

In order to compare the output power per unit volume of two DFBMs, the power losses will be used as a direct measure of the output power of the two motors. Moreover, as the copper loss is only a small percentage of the total losses in these motors, one can take the core loss as an indication of the output power per unit volume of two motors. In other words, it is assumed that the small core loss of the motor will have the large output power per unit volume.

To allow for consistent performance comparison, three-phase symmetrical currents are fed into the stator windings. The procedures to compare the performances of different motors are:

1) Perform synchronous operation simulation. If the magnitude of the computed electromagnetic torque of the torque-angle curve is high, it has high torque density.

2) Perform double-fed operation simulation to compute the full-load torque, back EMF and core losses using transient 2D FEM. The core losses of the two motors are computed by using the method presented in [14-18].

3. System Structure of Two DFBMs

Fig. 1(a) and Fig. 1(b) show the cross section of DFBM-I and DFBM-II respectively. The DFBM system of the two motors are the same configuration, as shown in Fig. 2, the DFBM system consists of three main components, a DFBM, a back-to-back inverter and an associated controller. DFBM is a controlled electric machine, and it is necessary to mate DFBM with a bidirectional power flow converter.

In the system, the stator of a DFBM has two sets of three-phase sinusoidal distributed windings. One set of windings is connected directly to the power grid. The other set of windings is fed with variable voltages at variable frequencies from a converter that also is connected to the power grid. The two sets of windings differ in pole numbers, one of $2p$ and another $2q$. The rotor of the DFBM is a special design, its pole number is p_r, and

$$p_r = p+q, \tag{1}$$

The operation of the DFBM relies on the interaction of the two stator windings through the intermediate action of the rotor. When one set of symmetrical sine-wave currents of frequency f_1 are flowing in $2p$ pole number windings, a set of three-phase back EMFs will be induced with a frequency of f_2 in the $2q$ pole number windings. The two electrical frequencies f_1 and f_2 are related to the rotor mechanical speed nrm by the following equation:

$$n_{rm} = 60\ (f_1 \pm f_2) / p_r, \quad (2)$$

Electromechanical energy conversion will take place in DFBMs if Eq. (2) is satisfied. For the proposed DFBM, the parameters are $2p$=8, $2q$=22, and p_r =15; f_1 =50 Hz and f_2 = 35 Hz. The rotating speed of the rotor is 60 rpm. The main dimensions of DFBM-I and DFBM-II are listed in Table 1 and Table 2 respectively. The stator of the two DFBMs is designed with 36 slots, and the single-layer full-pitch of 8-pole and 22-pole stator winding connections is shown in Fig. 3(a) and Fig. 3(b) respectively.

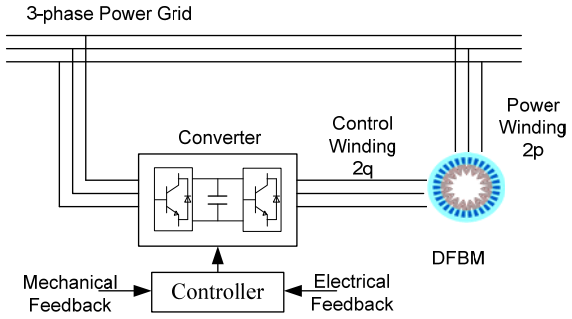

Fig. 2. Schematic diagram of a DFBM system.

Table 1. Main dimensions of DFBM-I.

Stator OD (mm)	300	Rotor OD (mm)	199
Stator ID (mm)	200	Rotor ID (mm)	50
Stator slots	36	Airgap length (mm)	0.5
Stack length (mm)	500	Speed of rotor (rpm)	60
Rotor pole number	15	Stator pole number	8, 22

Table 2. Main dimensions of DFBM-II.

Outer stator OD (mm)	300	Inner stator OD (mm)	206
Outer stator ID (mm)	220	Stack length (mm)	500
Two stator slots	36	Inner stator pole number	8
Speed of rotor (rpm)	60	Outer stator pole number	22
Airgap length (mm)	0.5	Steel segments length (mm)	15

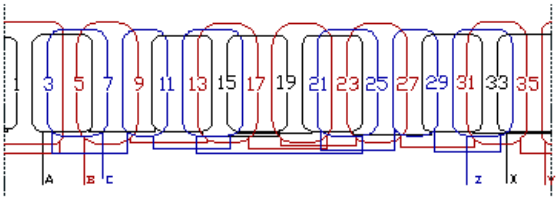

(a) 8 pole number stator winding with 36 slots

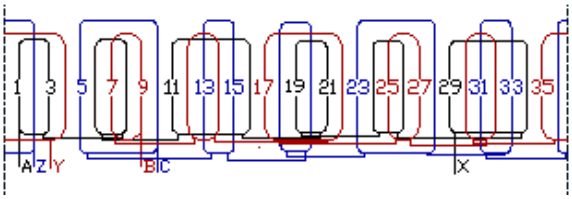

(b) 22 pole number stator winding with 36 slots

Fig. 3. Stator windings connection.

4. Performance Analysis by FEM

4.1. Two DFBMs Running on Synchronous Operation

In Eq. 2, depending on the value of controlled frequency f_2, a DFBM can operate in three modes: sub-synchronous operation (f_2 < 0), synchronous operation (f_2 = 0, with dc excitation) and super-synchronous operation (f_2 > 0). The synchronous, doubly-excited mode in which f_2=0, is straightforward and will be used as the starting point for analysis in the paper.

The direction of power flow in the control (secondary) winding depends on the operation modes of the drive system. The quadrants in this context are defined by the zero torque axis and the control winding frequency on the horizontal axis, with 0 Hz indicating DC at the natural synchronous speed, as shown in Fig. 4, the direction of converter power flow has been indicated using sign + for power flowing into the control winding, and sign – for power flowing out.

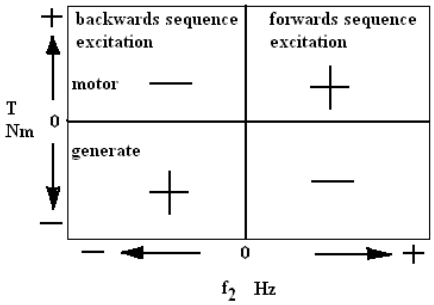

Fig. 4. Power flow in the control (secondary) winding.

Two-dimensional (2-D) transient finite element method (FEM) is employed to analyze the proposed DFBMs, the advantages of the transient FEM is that the realistic conditions of lamination geometries, core materials, and winding connections are all considered collectively and faithfully. The magnetic flux distribution of the DFBM-I and DFBM-II at natural synchronous condition can be investigated when one of the two sets of stator windings is excited with a three-phase current at 50 Hz. The other set of stator windings are fed with three-phase DC currents, and the rotor speed is 200rpm. The flux distribution over the cross-section of the DFBM-I and DFBM-II are shown in Fig. 5 and Fig. 6 respectively. Fig. 5(a) is the flux density in the DFBM-I, and Fig. 5(b) is the distribution of magnetic lines as well as Fig. 6(a) and Fig. 6(b). The air-gap field distribution and its harmonic spectra of the two DFBMs with fractional-slot windings are shown in Fig. 7 and Fig. 8 respectively. In DFBM-II, there are two air-gaps on both sides of modulation steels.

It is noted that the 15 pole-pair harmonic (Fig. 7 and Fig. 8) is larger than other harmonics because of the presence of modulation steels, and its magnitude

of DFBM-I is larger than that of DFBM-II. This 15 pole-pair harmonic is the functional harmonic for power conversion. Indeed one of the main optimization objectives of the study is to enhance the operational harmonics and suppress the other harmonics. The dimensions of the modulation steels, the number of pole-pairs of the windings, the length of the air-gap and the shape of the slots are factors governing the harmonic distribution of the flux density.

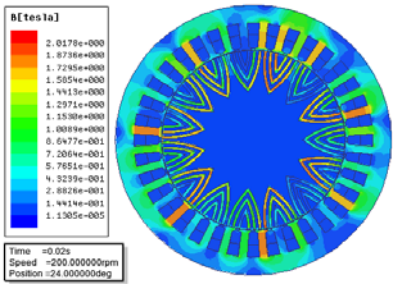

(a) Flux density in the DFBM-I

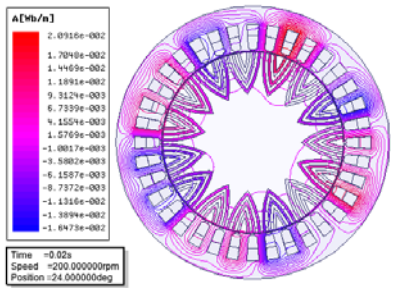

(b) Distribution of magnetic lines in the DFBM-I

Fig. 5. Flux distribution of DFBM-I.

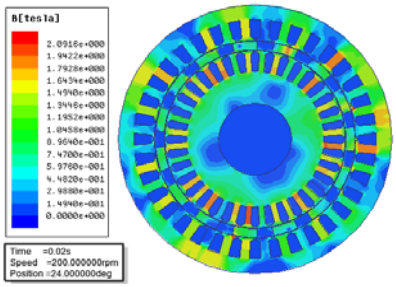

(a) Flux density in the DFBM-II

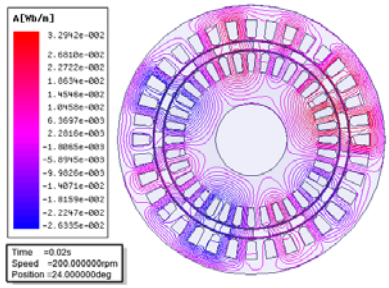

(b) Distribution of magnetic lines in the DFBM-II

Fig. 6. Flux distribution of DFBM-II.

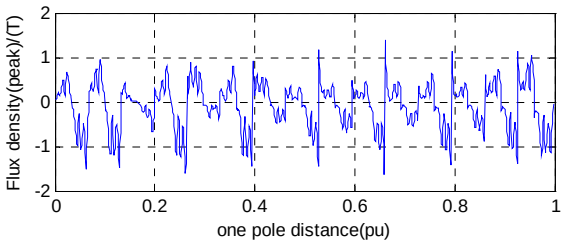

(a) Airgap-flux density

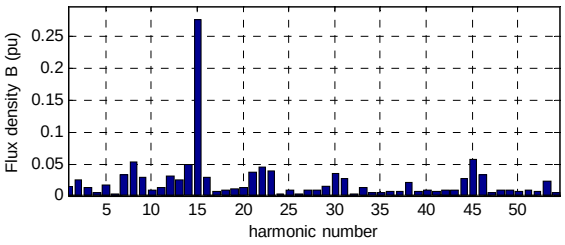

(b) Harmonics

Fig. 7. Air-gap flux density waveform and its harmonics of DFBM-I.

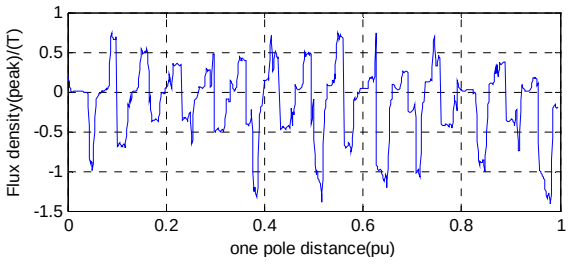

Fig. 8 (a). Air-gap flux density waveform and its harmonics of DFBM-II: Flux density for outer air-gap.

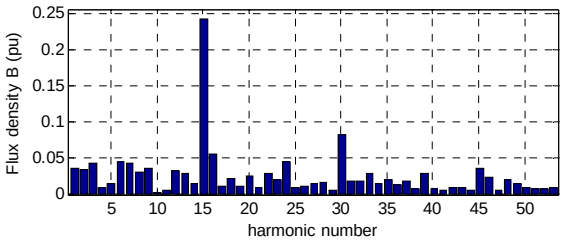

Fig. 8 (b). Air-gap flux density waveform and its harmonics of DFBM-II: Harmonics for outer air-gap.

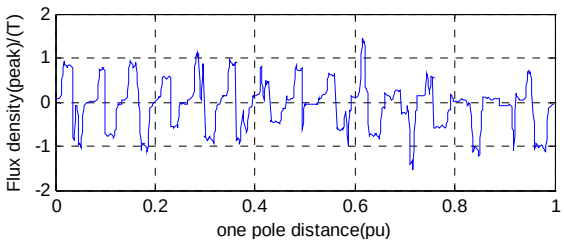

Fig. 8 (c). Air-gap flux density waveform and its harmonics of DFBM-II: Flux density for inner air-gap.

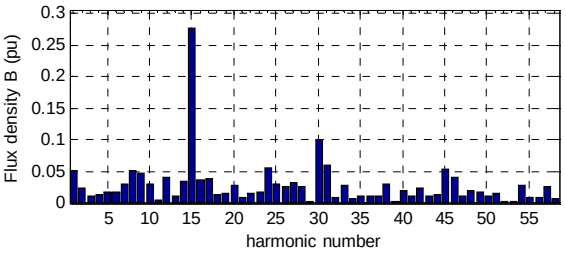

Fig. 8 (d). Air-gap flux density waveform and its harmonics of DFBM-II: Harmonics for inner air-gap

In DFBM, when one set of stator winding is excited by DC or AC, Back EMF voltages will be induced in another set of stator windings, due to mechanical rotation of the rotor. If a set of currents of the same frequency as that of the mutual flux linkage variation are injected into the second set of stator windings, the electromagnetic torque will be produced.

The torque production by finite element analysis is directly based on the magnetic field density and intensity on each element. The results are considered accurate because the complicated geometry of the FM-DFBG and nonlinearity of the materials are full considered. Fig. 9 shows the torque production curves computed directly by finite element method of the DFBM-I and DFBM-II. In Fig. 9, the average torque of two DFBMs is about 169 Nm and 171 Nm respectively. Therefore the torque density of DFBM-II is larger than that of DFBM-I.

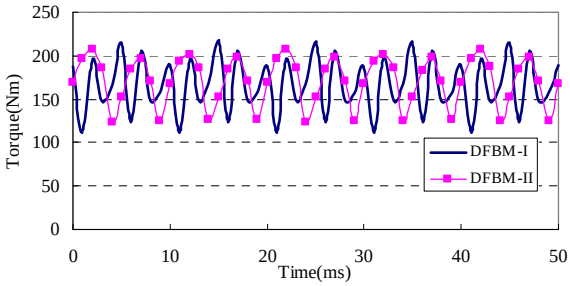

Fig. 9. Torque versus time of two DFBMs.

4.2. Two DFBMs Running on Double-fed Operation

In DFBM, when two sets of stator windings are excited by 50 Hz and 35 Hz AC currents respectively, the machine is running on double-fed operation, and the rotor speed is 60 rpm. By the same method, we have also investigated flux distribution, torque capability, core losses and efficiency of DFBM-I and DFBM-II.

Fig. 10(a) and Fig. 10(b) show the computed torque as a function of the rotor angles for DFBM-I and DFBM-II respectively. In Fig. 10, the maximum torque of the two DFBMs is the same, DFBM-I is about 172 Nm, DFBM-II is about 171 Nm.

As shown in Fig. 11, core losses of two DFBMs with factional-slot stator windings have been analyzed as well. It can be observed that the core losses of DFBM-II is larger than that of DFBM-I, and it is about 240 W for DFBM-I, 380 W for DFBM-II. The copper losses of two motors are 21 W, then the efficiency of two motors can be calculated, 92.2% for DFBM-I, 90 % for DFBM-II. According to the comparison rules, the power density of DFBM-I is larger than that of DFBM-II.

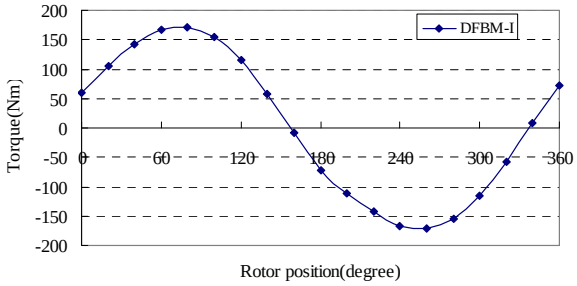

(a) DFBM-I

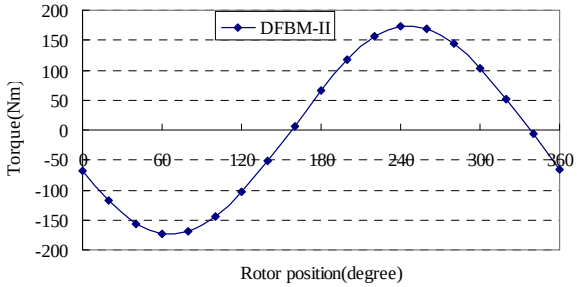

(b) DFBM-II

Fig. 10. Torque-angle curve of two DFBMs running on double fed operation.

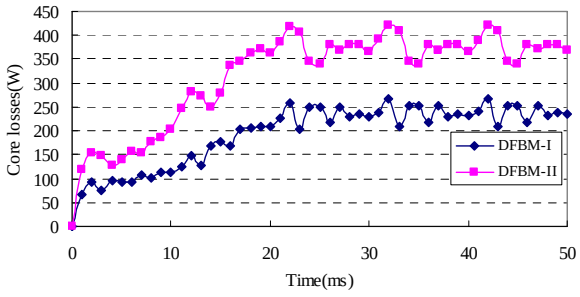

Fig. 11. Core losses of two DFBMs.

7. Conclusions

The paper focuses on the performances comparison analysis of two topologies of low-speed double-fed brushless machine (DFBM) with 36 slots fractional slot windings. To fairly compare the torque capability and power efficiency of two topologies DFBMs, some comparison rules are presented, and

the flux distribution, the flux density in air-gap, electromagnetic torque, core losses and efficiency of two DFBMs running on synchronous and double-fed operations have been investigated by using 2D transient finite element analysis method. All studies show that the torque density of DFBM-II is larger than that of DFBM-I, the power density of DFBM-I is larger than that of DFBM-II. Two DFBMs with fractional-slot windings are potential to achieve high efficiency and apply in double-fed low-speed drive applications.

Acknowledgements

This work was supported by the National Natural Science Foundation of China (No. 51377008).

References

[1]. R. Pena, J. C. Clare, and G. M. Asher, Doubly fed induction generator using back-to-back PWM converters and its application to variable speed wind-energy generation, *IEE Proceedings on Electric Power Applications*, Vol. 143, Issue 3, May 1996, pp. 231–241.

[2]. R. Pena, R. Cardenas, J. Proboste, J. Clare, and G. Asher, Wind-Diesel Generation Using Doubly Fed Induction Machines, *IEEE Transaction on Energy Conversion*, Vol. 23, Issue 1, Mar. 2008, pp. 202–214.

[3]. L. J. Hunt, The cascade induction motor, *Journal of IEE*, Vol. 52, 1914, pp. 406-426.

[4]. F. Creedy, Some developments in multi-speed cascade induction motors, *Journal of IEEE*, Vol. 59, 1921, pp. 551-552.

[5]. L. Xu, F. Liang and T. A. Lipo, Transient model of a doubly excited reluctance motor, *IEEE Transactions on Energy Conversion*, Vol. 6, Issue 1, March 1991, pp. 126-133.

[6]. L. Xu, Analysis of a doubly-excited brushless reluctance machine by finite element method, in *Proceedings of the IEEE Industry Application Society Annual Meeting*, Houston, 1992, Vol. 1, pp. 171-177.

[7]. H. Liu and L. Xu, Comparison study of doubly excited brushless reluctance machine with different rotor pole numbers, in *Proceedings of the International Conference on Power Electronics and Motion Control (IPEMC' 09)*, Wuhan, China, 17-20 May 2009, pp. 830-835.

[8]. K. Atallah, S. D. Calverley and D. Howe, Design, analysis and realization of a high-performance magnetic gear, *IEE Proceedings on Electric Power Applications*, Vol. 151, Issue 2, March 2004, pp. 135-143.

[9]. K. Atallah and D. Howe, A novel high-performance magnetic gear, *IEEE Transactions on Magnetics*, Vol. 37, Issue 4, Part 1, July 2001, pp. 2844-2846.

[10]. P. O. Rasmussen, T. O. Andersen, F. T. Jorgensen, O. Nielsen, Development of a high-performance magnetic gear, *IEEE Transactions on Industry Applications*, Vol. 41, Issue 3, May-June 2005, pp. 764-770.

[11]. M. Aubertin, A. Tounzi and Y. Le Menach, Study of an electromagnetic gearbox involving two permanent magnet synchronous machines using 3-D-FEM, *IEEE Transactions on Magnetics*, Vol. 44, Issue 11, Part 2, November 2008, pp. 4381-4384.

[12]. K. Atallah, J. Rens, S. Mezani, and D. Howe, A novel 'pseudo' direct drive brushless permanent magnet machine, *IEEE Transactions on Magnetics*, Vol. 44, Issue 11, 2008, pp. 4349-4352.

[13]. L. Jian, K. T. Chau and J. Z. Jiang, A magnetic-geared outer-rotor permanent-magnet brushless machine for wind power generation, *IEEE Transactions on Industry Applications*, Vol. 45, Issue 3, May-June 2009, pp. 954-962.

[14]. D. Lin, P. Zhou, W. N. Fu, Z. Badics and Z. J. Cendes, A dynamic core loss model for soft ferromagnetic and power ferrite materials in transient finite element analysis, *IEEE Transactions on Magnetics*, Vol. 40, Issue 2, March 2004, pp. 1318-1321.

[15]. H. Jussila, P. Salminen, M. Niemela, and J. Pyrhonen, Guidelines for designing concentrated winding fractional slot permanent magnet machines, in *Proceedings of the International Conference on Power Engineering, Energy and Electrical Drives*, Setubal, Portugal, April 2007, pp. 191–194.

[16]. N. Bianchi, S. Bolognani, and E. Fornasiero, A general approach to determine the rotor losses in three-phase fractional-slot PM machines, in *Proceedings of the IEEE International Conference on Electric Machines & Drives*, Antalya, May 3–5, 2007, Vol. 1, pp. 634–641.

[17]. N. Bianchi, M. D. Pr´e, G. Grezzani, and S. Bolognani, Design considerations on fractional-slot fault-tolerant synchronous motors, *IEEE Transactions on Industry Applications*, Vol. 42, Issue 4, 2006, pp. 997–1006.

[18]. A. El-Refaie, Z. Zhu, T. Jahns, and D. Howe, Winding inductances of fractional slot surface-mounted permanent magnet brushless machines, in *Proceedings of the IEEE Industry Applications Society Annual Meeting*, Edmonton, Alta, October 5–9, 2008, pp. 1–8.